

NUMERICAL ANALYSIS OF INJECTION PARAMETERS INFLUENCE ON DIESEL ENGINE PERFORMANCES AND EMISSIONS CORRELATED BY MAXIMUM IN-CYLINDER PRESSURE

by

**Mohamed BENCHERIF^{a,b*}, Tewfik LEFTAS^{a,c},
and Nasreddine LARBES^{a,c}**

^a Department of Mechanical Engineering, USTO-MB,
El M'naouar Oran, Algeria

^b LTE Laboratory, ENPO-MA, El M'naouar Oran, Algeria

^c Applied Mechanics Laboratory (LMA), USTO-MB,
El M'naouar Oran, Algeria

Original scientific paper

<https://doi.org/10.2298/TSCI220120017B>

The present work deals with a numerical investigation on an experimental single cylinder direct injection Diesel engine. Calculations are carried out with Kiva3v2 code using multidimensional detailed chemistry. The study was carried out on predicted CO, and NO_x emission levels by the engine cylinder before exhaust valve opening. Correlations proposed for predicted NO, CO, and NO_x levels function of fuel, O₂, N₂ concentrations and the maximum in-cylinder pressure rather than temperature. Predicted values of averaged pressures, O₂, CO, and CO₂ levels in the exhaust manifold were validated by the measured ones for a set of five loads at 1500 rpm. CO, NO, and NO_x concentrations at the exhaust obtained by calculations lies perfectly with measured values. Otherwise, numerical simulations lead us to analyze injection timing, duration and fuel amount injected effect on the engine performances, ignition delay, combustion duration as well as CO and NO_x emission levels.

Key words: *modelling, correlations, Kiva3v2, CO, NO_x, in-cylinder pressure, injection parameters, injection delay, combustion duration*

Introduction

It is well known that thermal engine performances enhancement depends on combustion, turbulence and spray understanding in addition emission levels reduction at the exhaust [1, 2]. Combustion process in internal engines has been the major objective for several mathematical, numerical and comprehensive models developers and scientific researchers [3-6]. Progress in Diesel engines combustion phenomena modelling grows with CFD tools evolution. Indeed, suitable accuracy can be obtained with CFD tools which represent an alternate way to investigate and analyze complex 3-D configurations using RANS transport equations system and Arbitrary Lagrangian – Eulerian method coupled at sub-models for combustion, combustion-turbulence interactions, and diphasic injection [7-10]. Chemical kinetics and equilibrium state combustion aspect can be taken into account with reaction mechanisms. Physical parameters related to the dynamics of the two-phase jet as well as the chemical parameters occur-

* Corresponding author, e-mail: mohamed.bencherif@univ-usto.dz

ring at a sub-mesh scale are treated by sub-models from an in-like calculation cell mesh scale [11-16]. The NO_x emitted by conventional diesel [17] and biodiesel fueled engines [18, 19] remains the main chemical pollutant targeted by reserchers in the world.

In the present work, algebraic relationships for CO, NO, and NO_x concentrations calculated exactly at the exhaust phase start have been established. Because of his cetane number (~ 50) C_7H_{16} is suggested as fuel for diesel engine simulations [1, 2, 20-22]. Indeed, exhaust phase occur to late diffusion combustion characterized by equilibrium combustion where [CO], [NO], and [NO_x] seems to be constant. Thus, $d[\text{CO}]/dt$, values are function of [C_7H_{16}], [O_2], [CO], and [CO_2] levels, and both $d[\text{NO}]/dt$ and $d[\text{NO}_x]/dt$ values are function of [C_7H_{16}], [O_2], [N_2] levels in the exhaust gases as well as the maximal in-cylinder averaged pressure rather than the maximal in-cylinder averaged temperature proposed in [22]. Reduced mechanism composed of a global reaction for C_7H_{16} associate to 245 elementary reactions with a set of 60 species has been used. Concentrations of O_2 , CO, and CO_2 calculated at the exhaust have been validated by the measured values.

The NO and CO rates modelling

It is well known that the thermal NO concentration can be predicted using three elementary reactions of Zeldovich mechanism. A set of six reaction coefficients functions of the static temperature are to be calculated each time step. The $d[\text{NO}]/dt$ given by a first order differential equation and [O_2], [N_2], [O], [N], [OH], [H], and [NO] are estimated and five additional equations (partial equilibrium OHC) are added in the aim to estimate [O_2], [O], [OH], and [H]. simplifications by neglecting slow reverse reactions can be done if one suppose steady and partial equilibrium states. The $d[\text{NO}]/dt$ can determine according to Bockhorn relationships [4]:

$$\frac{d[\text{NO}]}{dt} = 4.710^{13} \exp\left[-\frac{67837}{T}\right] [\text{N}_2] \sqrt{[\text{O}_2]} \quad (1)$$

Or Kee *et al.* [23] relationship:

$$\frac{d[\text{NO}]}{dt} = 1.310^{15} \exp\left[-\frac{75500}{T}\right] [\text{N}_2] \sqrt{[\text{O}_2]} \quad (2)$$

Similarly, according to Heywood [3, 23] one can determine $d[\text{NO}]/dt$ by mean of burned gases fraction temperature T :

$$\frac{d[\text{NO}]}{dt} = \frac{610^{16}}{T} \exp\left[-\frac{69090}{T}\right] [\text{N}_2] \sqrt{[\text{O}_2]} \quad (3)$$

suming steady-state and partial equilibrium chemistry assumptions an analogous relation given by Dryer and Glassman [24] for CO concentration rate using global dissociation reaction with the relationship:

$$\frac{d[\text{CO}]}{dt} = A_{\text{CO}} \exp\left[-\frac{20130}{T}\right] [\text{CO}] [\text{O}_2]^{0.25} \sqrt{[\text{H}_2\text{O}]} \quad (4)$$

with $A_{\text{CO}} = -1.3 \cdot 10^{10}$.

In a previous work [22] the authors new correlations for predicting NO and NO_x levels at late diffusion combustion phase in the exhaust of an experimental engine have been carried

out from a multidimensional detailed chemistry simulation. Both concentrations of NO and NO_x have been estimated using fuel, N₂, O₂ concentrations and maximal in-cylinder temperature by the relations:

$$\frac{d[\text{NO}]}{dt} = 10^{13} [\text{N}_2][\text{Fuel}]\sqrt{[\text{O}_2]} \exp\left[-\frac{A}{T_{\max}^\alpha}\right] \quad (5)$$

$$\frac{d[\text{NO}_x]}{dt} = 10^{13} [\text{N}_2][\text{Fuel}]\sqrt{[\text{O}_2]} \exp\left[-\frac{B}{T_{\max}^\alpha}\right] \quad (6)$$

where

$$A = 690 \text{ 1/K}, B = 780 \text{ 1/K}, \text{ and } \alpha = 0.362$$

Multidimensional turbulent flow and detailed chemistry modelling

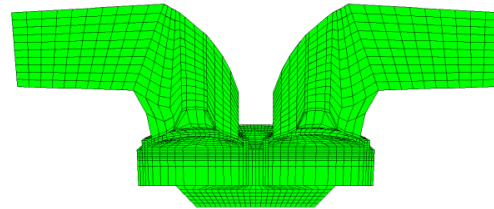
Commonly, simulating physical phenomena as turbulent combustion of a multi-species mixture in a compression ignition engine can be successfully done by the resolution of the RANS system. It is principally composed by species and global mass conservation, momentum conservation, energy conservation, and the equation of the state. It also represents the Eulerian flow phase. The diphasic fl spray with breakup, coalescence, and evaporation of fuel droplets during the Lagrangian phase can be performed with the Taylor analogy break-up model (TAB) developed by Reitz [16]. There are two regimes controlling the breakup process of the droplets, bag breakup and stripping breakup. The breakup rate of the droplet is calculated for each one and the instability is determined by the mean of the Weber number. Break-up associated characteristic time is then determined for both regimes [15, 16]. Source terms due, respectively to heat released by chemical reactions and the spray/flow interaction are calculated in a parallel Lagrangian phase. For the overall chemical mechanism, chemical source term, heat balance for each reaction, the reaction rate and each kinetic reaction constant are estimated separately for each calculation cell when the averaged cell temperature is greater than 900 K. Adapted version of Kiva3v2 with a new combustion-turbulence sub-model proposed by Golovitchev *et al.* [1] and Nordin [2] has been used. The new sub-model integrated into Kiva3v2 version is essentially based on the generalized partially stirred reactor model [20-22]. Turbulence model used is the modified RNG (*k-ε*) model.

Experimental facilities

Measures are done on a test bench and the exhaust gases analyzer. Chemical species sensors and accuracies can be shown in the tab. 1. The experimental engine is a one cylinder direct injection Diesel engine implanted in the energetic and environment systems department (DSEE) IMT ex école des mines de Nantes. Cases treated concern five loads at engine speed of 1500 rpm. The engine has been widely explored by a great number of experimental and numerical studies as well as combustion-turbulence interactions [20-22] extraction of NO_x and NO correlations [20], improving engine performances and reducing NO_x levels using biofuels, animal fat emulsions [25], natural gas [26] and biogas [27]. The engine specifications are regrouped in tab. 1.

Table 1. Engine specifications

Designation	Value
Cylinder number	One cylinder
Engine speed	1500 rpm
Maximal power	5.4 kW at 1800 rpm
Piston diameter	9.525 cm
Piston Stroke	8.85 cm
Connecting rod length	16.5 cm
CR	18:1

**Figure 1. Numerical meshing (piston at 400 CA°)**

Mesh generation

The numerical grid mesh has been created with the Kiva3v preprocessing tool, Boundaries are labeled and much with real physical geometry of the piston, the bore, the stroke, the squish region and the intake and exhaust valves geometries. The grid is adjusted by the code performers and refinement of calculation mesh grid near the moving boundaries is achieved using 43 structured blocks. Total cell number of the numerical domain is 23000 cells with 26000 nodes. Figure 1 illustrates the computation grid before the exhaust valve opening. Three regions are considered distinctly the combustion chamber, the intake and the exhaust ports with their valves.

Results and discussions

The numerical test bench built in [22] is achieved by the following assumptions:

- For the validation of the in-cylinder averaged pressure, calculated values are picked from the combustion chamber (Region 1).
- Calculated values of $[O_2]$, $[CO]$, and $[CO_2]$ are taken from the exhaust volume (Region 3).

Validation and numerical test bench build

Figure 2 represents calculated and measured averaged in-cylinder pressure evolutions as well as the heat released [21]. Calculate mean in-cylinder pressure lie perfectly on the measured one. Discrepancies in the pressure prediction do not exceed 2% during compression combustion and expansion phases. According to a previous work presented by the authors the numerical code has been tuned in order to validate successfully CO, CO_2 , and O_2 concentrations. It has been shown that, for the five loads, measured values of $[O_2]$, $[CO]$ and $[CO_2]$ at the exhaust valve opening lies perfectly with those obtained by Kiva3v2 [19]. Thus, the tabulated chemistry used led to a suitable prediction of O_2 , CO, and CO_2 concentrations in the exhaust. Figure 3 illustrates confrontation between calculated values of $[O_2]$, $[CO]$, and $[CO_2]$ and those measured at the exhaust valve opening for both 80% and full load. It can be noted that further results and information are presented in [19]. The injection parameters related for each load can be shown in tab. 2. Injection duration and the start of injection are located using measured injection pressure curves.

The $[CO]$, $[NO]$, and $[NO_x]$ modelling

It's well known that because the partial equilibrium and the steady-state $d[CO]/dt$, $d[NO]/dt$ and $d[NO_x]/dt$ are very small at late diffusion combustion followed by the exhaust valve opening. Therefore, one can considerate that their concentrations are function of:

- The $[CO]$, $[CO_2]$, $[N_2]$, $[O_2]$ [3-5, 19, 21].
- Maximal in-cylinder pressure rather than temperature as proposed in [19]. In fact, maximum value of the averaged in-cylinder pressure, like temperature, is a thermodynamic function but much easier to measure in addition. The correlations with the peak cycle pressure in the cylinder should be more useful for experiencers and researchers involved in comprehensive combustion and engine modelling.
- The $[C_7H_{16}]$ have to be added since fuel depletion between injection start and combustion end lead to more accurate models and a better apprehending during premixed and diffusive combustion phases can be obtained.

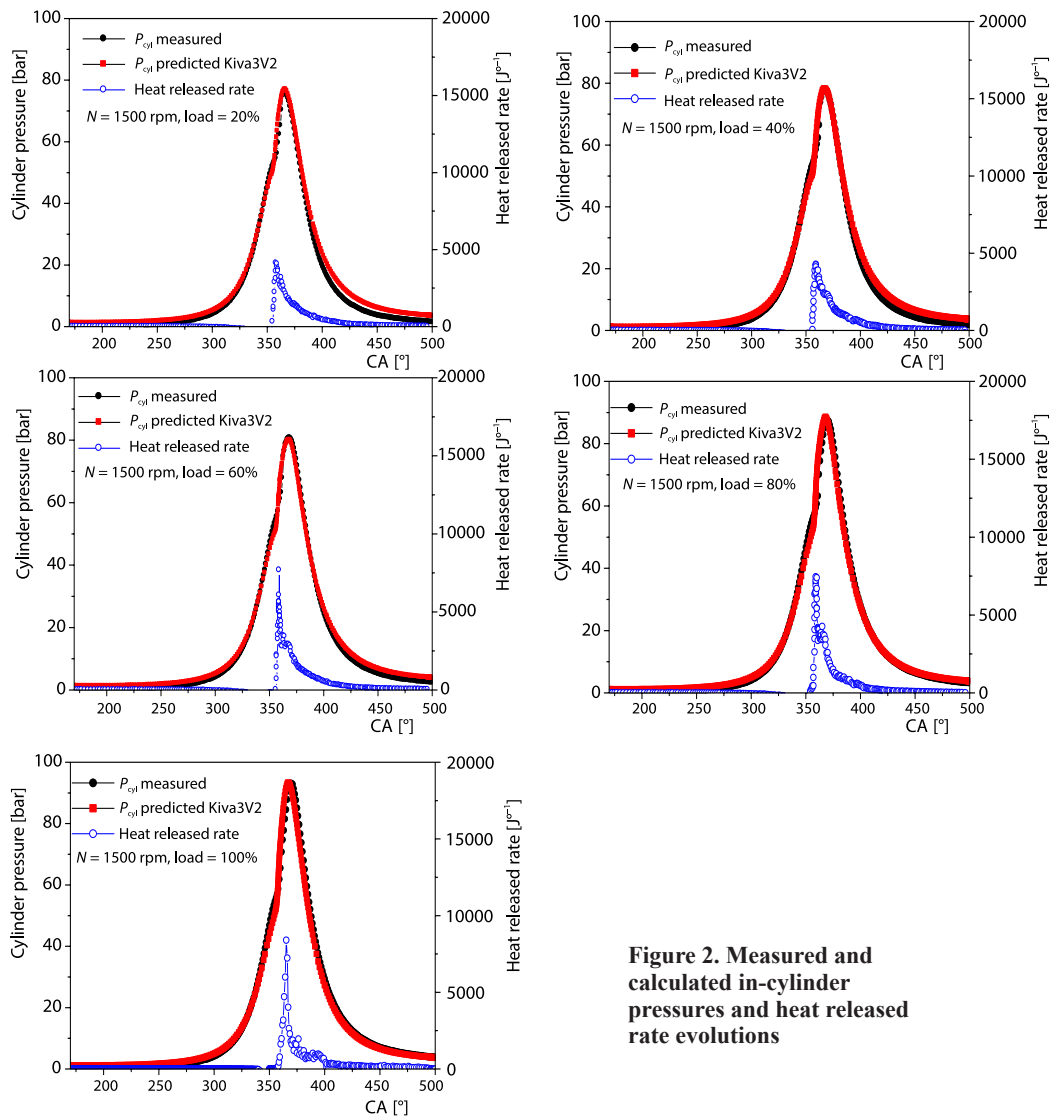
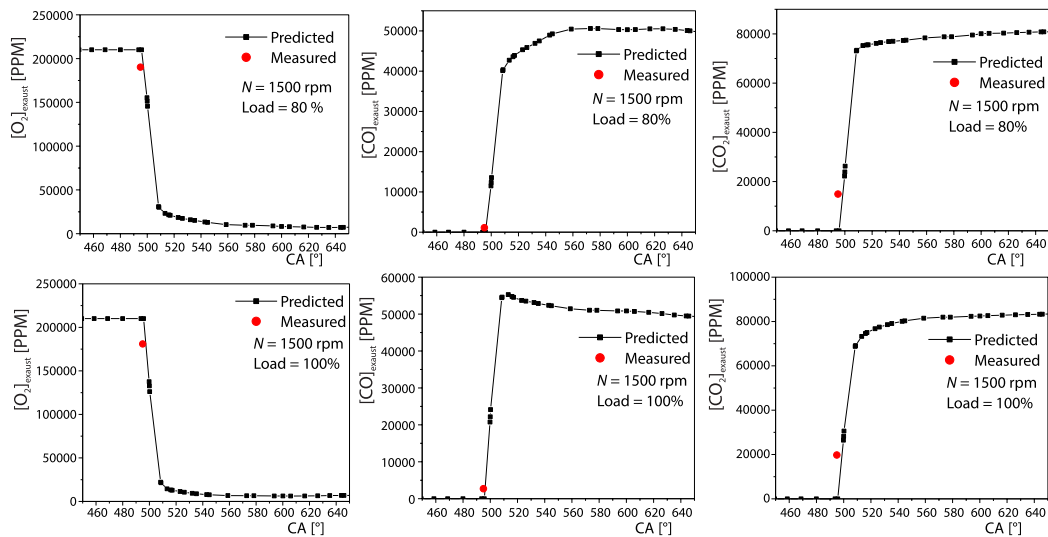


Figure 2. Measured and calculated in-cylinder pressures and heat released rate evolutions

Table 2. Injection parameters

Load	m_f	θ_{inj}	$\Delta\theta_{inj}$
%	mg/cycle	CA°	CA°
20	55	242	21
40	65		22
60	75		23
80	100		22
100	105		22

**Figure 3. Predicted and measured O₂, CO, and CO₂ concentrations in the exhaust region [19]**

The pressures unit in the following correlations is the Pascal. Thus:

$$\frac{d[\text{CO}]}{dt} = 2 \cdot 10^6 \exp\left[-\frac{20130}{P_{\max}}\right] [C_7H_{16}] [N_2] [O_2]^{0.25} [H_2O]^{0.5}$$

$$\frac{d[\text{NO}]}{dt} = \exp\left[-\frac{1480}{P_{\max}^{0.28}}\right] [C_7H_{16}] [O_2]^{0.5} [N_2] \quad (7)$$

$$\frac{d[\text{NO}_x]}{dt} = 10 A_{\text{NO}_x} \exp\left[-\frac{1500}{P_{\max}^{0.28}}\right] [C_7H_{16}] [O_2]^{0.5} [N_2]$$

Parametric analysis

The present section has been added to the paper in the attempt to bring a better understanding of the combustion process. Consequently, using numerical investigations, the analysis of influence of fuel mass injected, injection timing and injection duration on ignition delay, combustion duration and CO, NO, and NO_x concentrations in the exhaust has been carried-out.

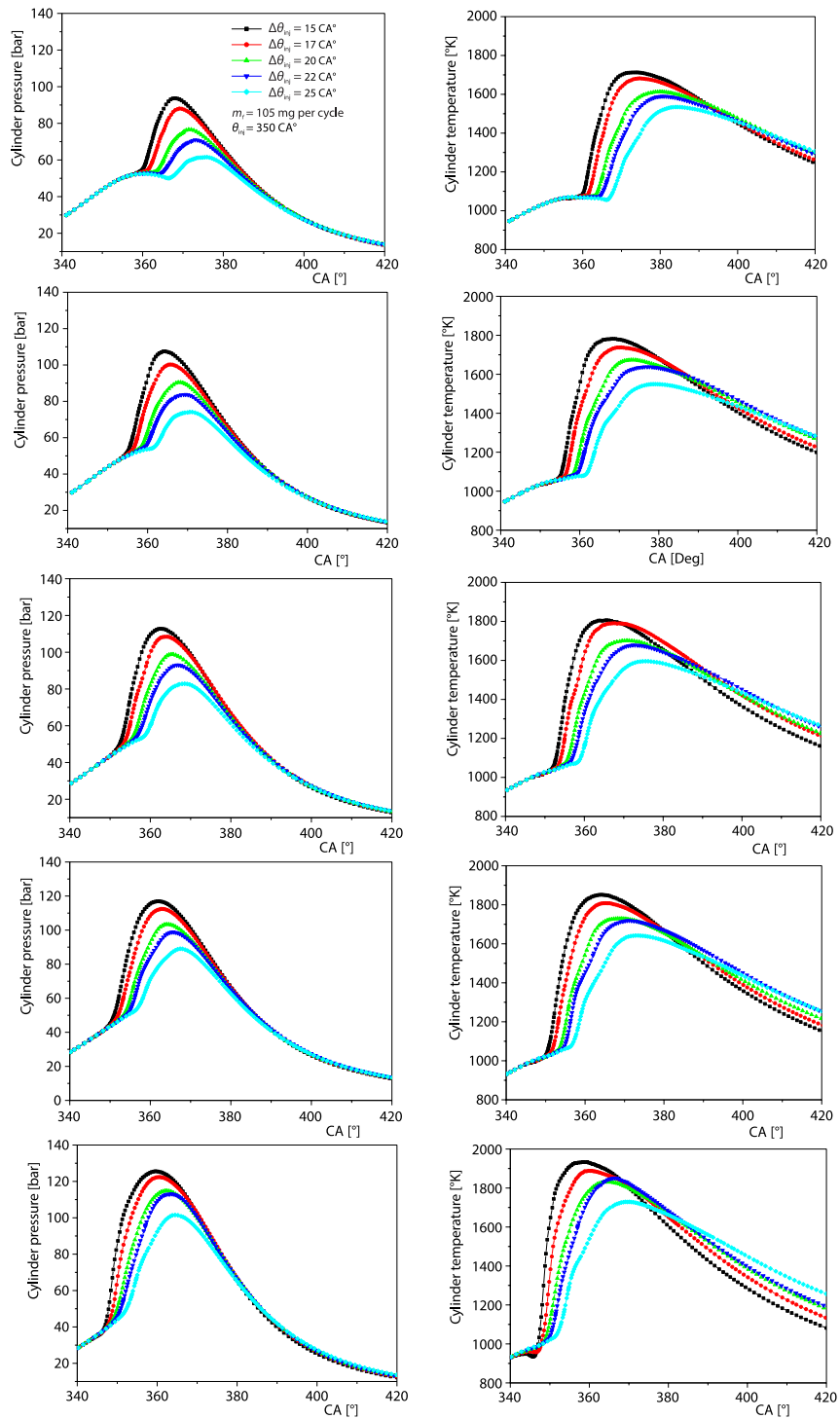


Figure 4. Averaged in-cylinder pressure and temperature evolutions for different injection timings and injection durations

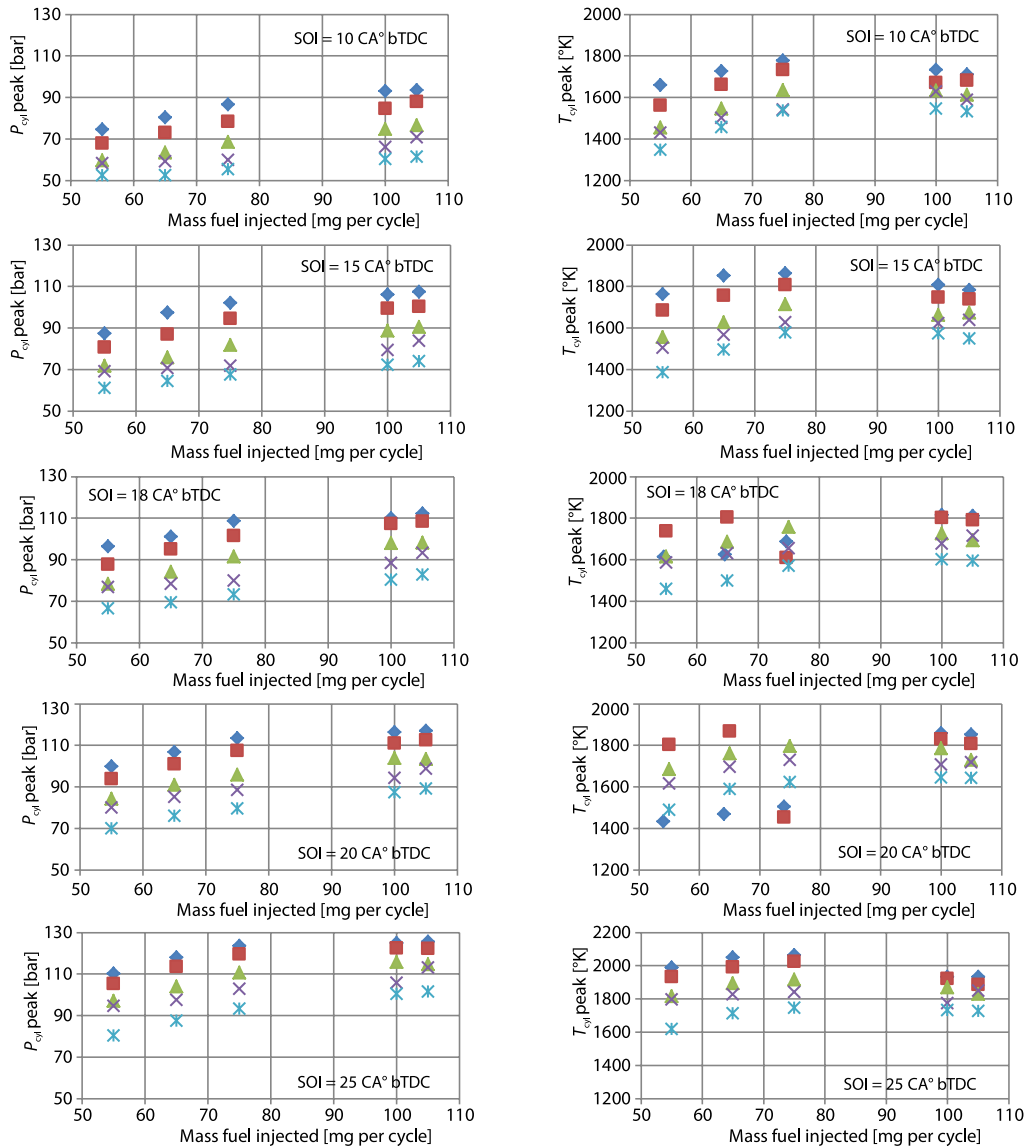


Figure 5. Averaged in-cylinder pressure and temperature peaks vs. mass fuel injected according to injection timing duration

Five different values of fuel mass injected, injection timing and injection duration have been tested with the calibrated version of the CFD code.

Actually, fuel masses injected are maintained as those in tab. 2 and for each value of the masse fuel injected, injection timing and injection duration have been varied, respectively, as follows:

Injection timing: 335 CA°, 340 CA°, 342 CA°, 345 CA° and 350 CA°.

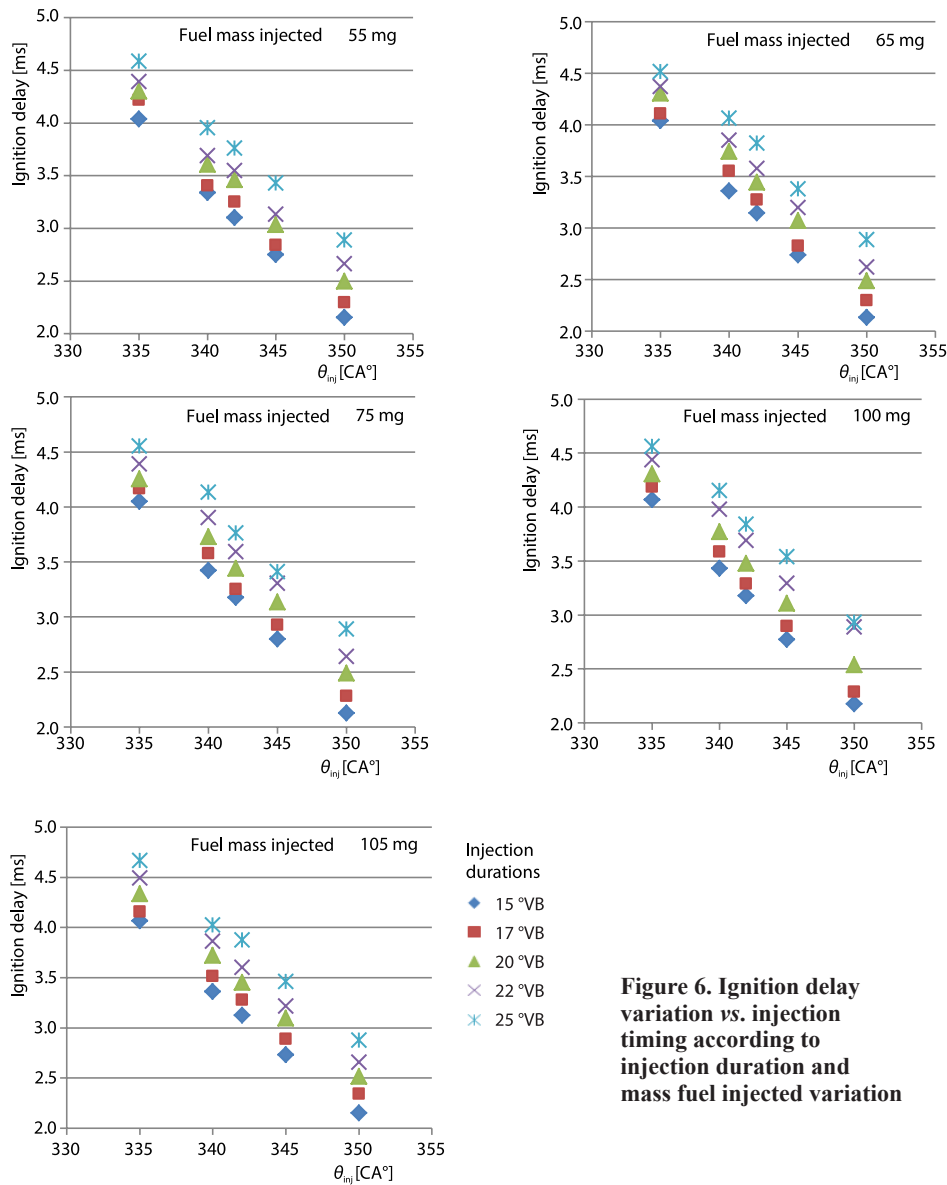


Figure 6. Ignition delay variation vs. injection timing according to injection duration and mass fuel injected variation

Injection duration: 25 CA°, 20 CA°, 17 CA°, 15 CA° as well as the specific value for each load in the validation so that 21 CA° when $m_f = 55$ mg/cycle, 22 CA° when $m_f = 65$ mg/cycle, 23 CA° when $m_f = 75$ mg/cycle, 22 CA° when $m_f = 100$ mg/cycle and 22 CA° when $m_f = 105$ mg/cycle. A combination of 125 cases has been achieved. Figure 4 presents in-cylinder pressure and temperature evolutions for combined injection timing and injection duration. Mass fuel injected is fixed to that of full load. For constant amount of fuel injected and constant injection timing increasing injection duration reduce the engine performances. But for constant amount of fuel injected and constant injection duration and increasing injection timing better

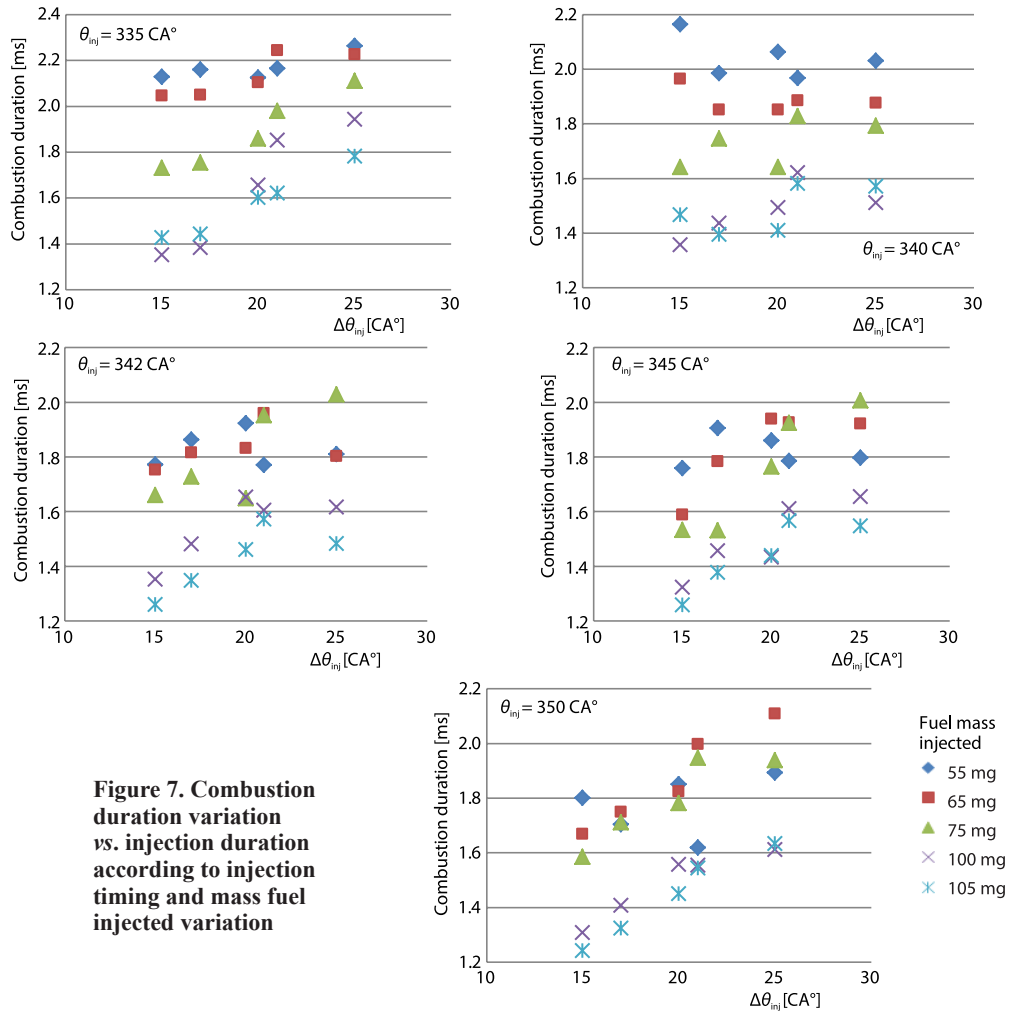


Figure 7. Combustion duration variation vs. injection duration according to injection timing and mass fuel injected variation

engine performances can be reached. Figure 5 illustrates averaged in-cylinder pressure and temperature peaks obtained for different injection timing, duration and mass fuel injected. Figures 6 and 7 present, respectively ignition delay and combustion duration according to different injection timing, duration and mass fuel injected. It has to be note that ignition delay lay on between the start of injection and combustion start. Combustion start and end have crank angles been calculated with the entropy variation according to Tazerout *et al.* method [28]. Ignition delay seems to be very sensitive to injection timing and injection duration variations. Otherwise, higher ignition delays are obtained with bigger amounts of fuel injected.

Figure 8 illustrates predicted CO and NO_x concentrations according to different injection timing when $m_f = 105 \text{ mg/cycle}$ and $\Delta\theta_{inj} = 22 \text{ CA}^\circ$.

As expected while engine performances increase considerably with the increase of injection timing however NO_x levels increase considerably about 5.6 times those obtained by late injection timing. In order to give useful results according to engine researchers and automotive engineers, NO_x and CO concentrations are illustrated in gr/Kwh unit instead of PPM.

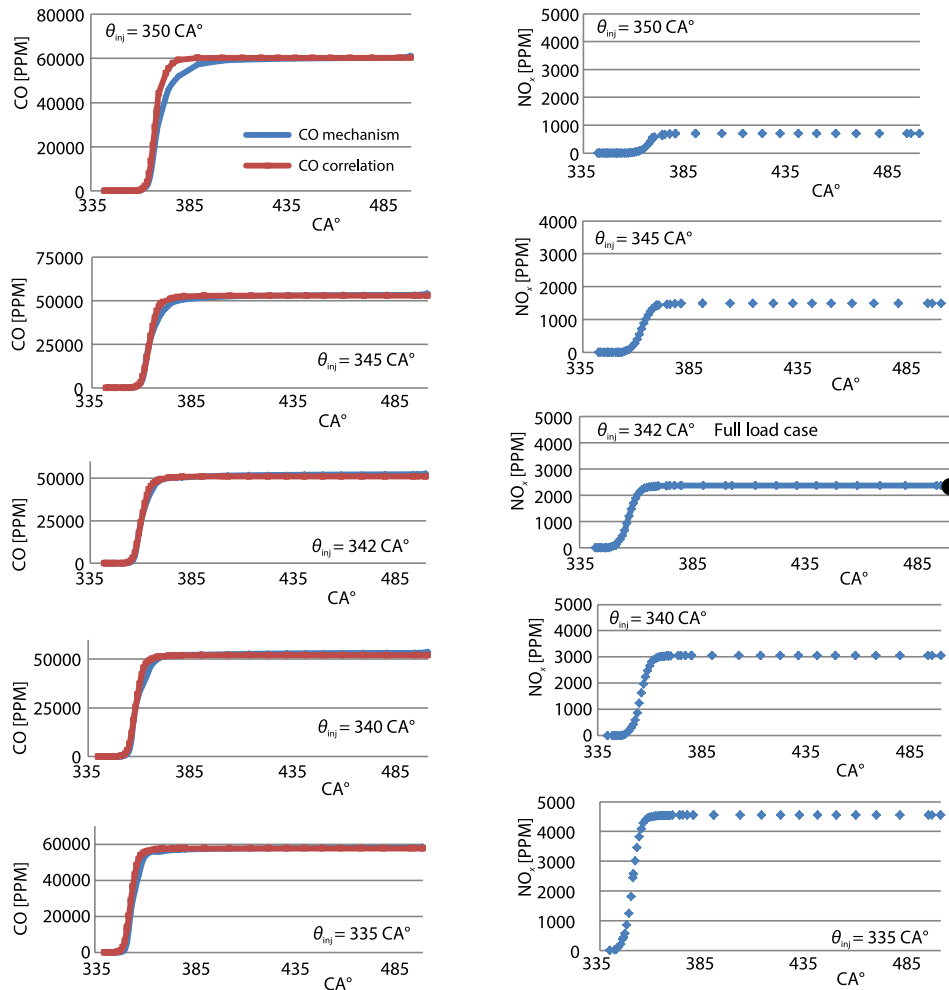


Figure 8. Predicted CO and NO_x concentrations according to different injection timing
 $m_f = 105 \text{ mg/cycle}$ and $\Delta\theta_{inj} = 22 \text{ CA}^\circ$

Figures 9 and 10 represent, respectively NO_x and CO concentrations for different injection parameters picked when exhaust valve is wide open. The figures summarize over all parametric cases studied. The NO_x levels increase considerably when mass fuel injected increased. For constant values of mass fuel injected late injection timing leads to huge NO_x levels and lower CO emissions. According to the results increasing the injection duration with fixed values of the mass of fuel injected per cycle seems to be efficient to reduce considerably the amount of NO_x at the exhaust however CO concentrations increase considerably.

Conclusions

A 3-D multidimensional numerical investigation was achieved using an adapted version of Kiva3v code. Reduced reaction mechanism of C₇H₁₆ has been used. As presented in a previous paper a numerical test bench have been build and used with the aim to improve algebraic correlations for NO, NO_x and CO concentrations emitted at the exhaust of an experimental

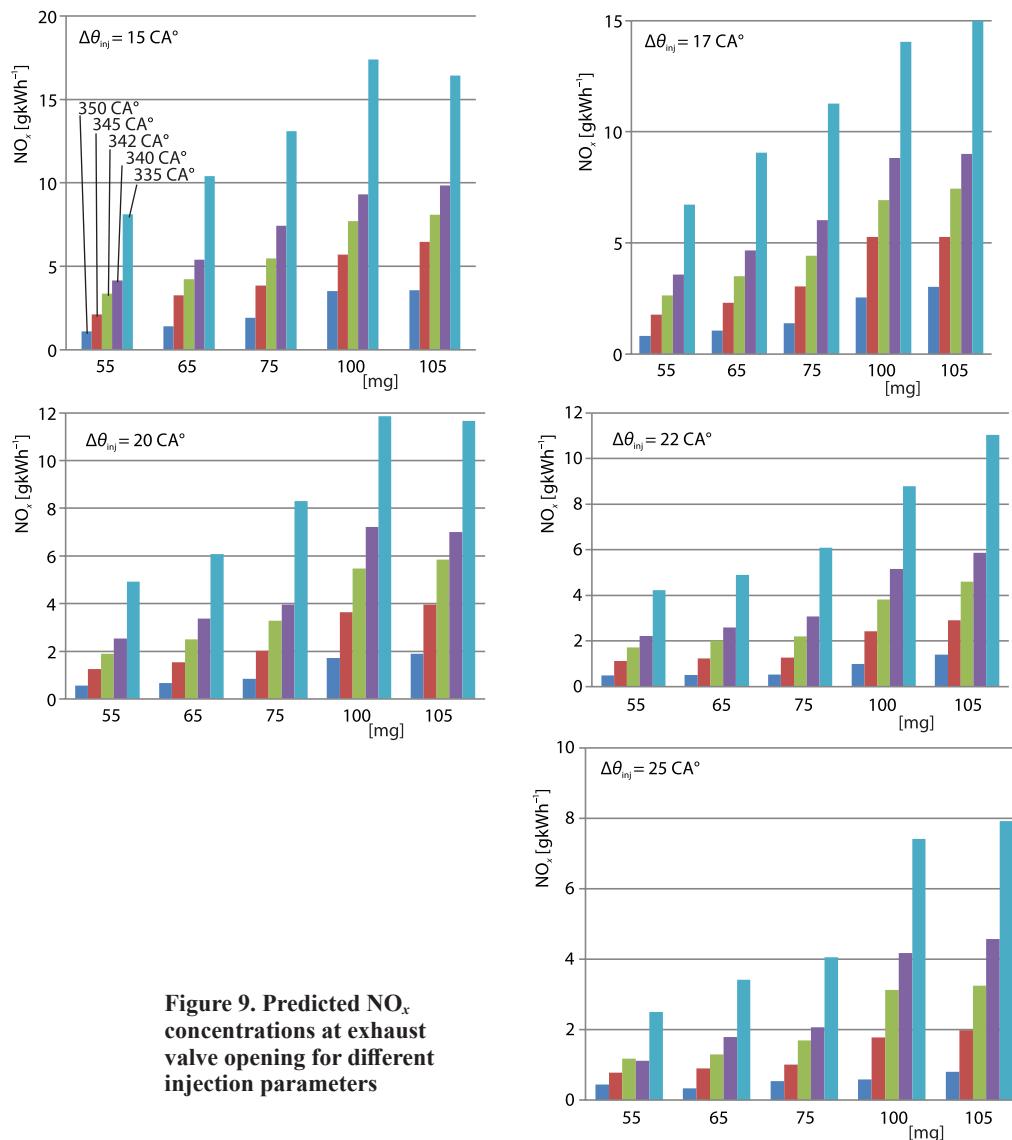


Figure 9. Predicted NO_x concentrations at exhaust valve opening for different injection parameters

direct injection diesel engine. Measured mean in-cylinder pressure, and O₂, CO, and CO₂ concentrations at the exhaust have been validated for five engine loads at 1500 rpm.

The principal originality of the correlations presented in this paper consists in the use of the maximum cylinder pressure rather than the maximum cylinder temperature. Indeed, the pressure is a thermodynamic function related to temperature but much more useful since it is easily measured on engine test bench. Otherwise, the correlations use fuel and measurable species concentrations O₂, N₂, H₂O, and CO₂.

A good agreement has been noted between predicted and measured CO, NO, and NO_x at the exhaust. In the attempt to optimize the studied engine, a parametric analysis on the injection timing and duration as well as the fuel mass injected per cycle influence on the engine performances and emissions is performed.

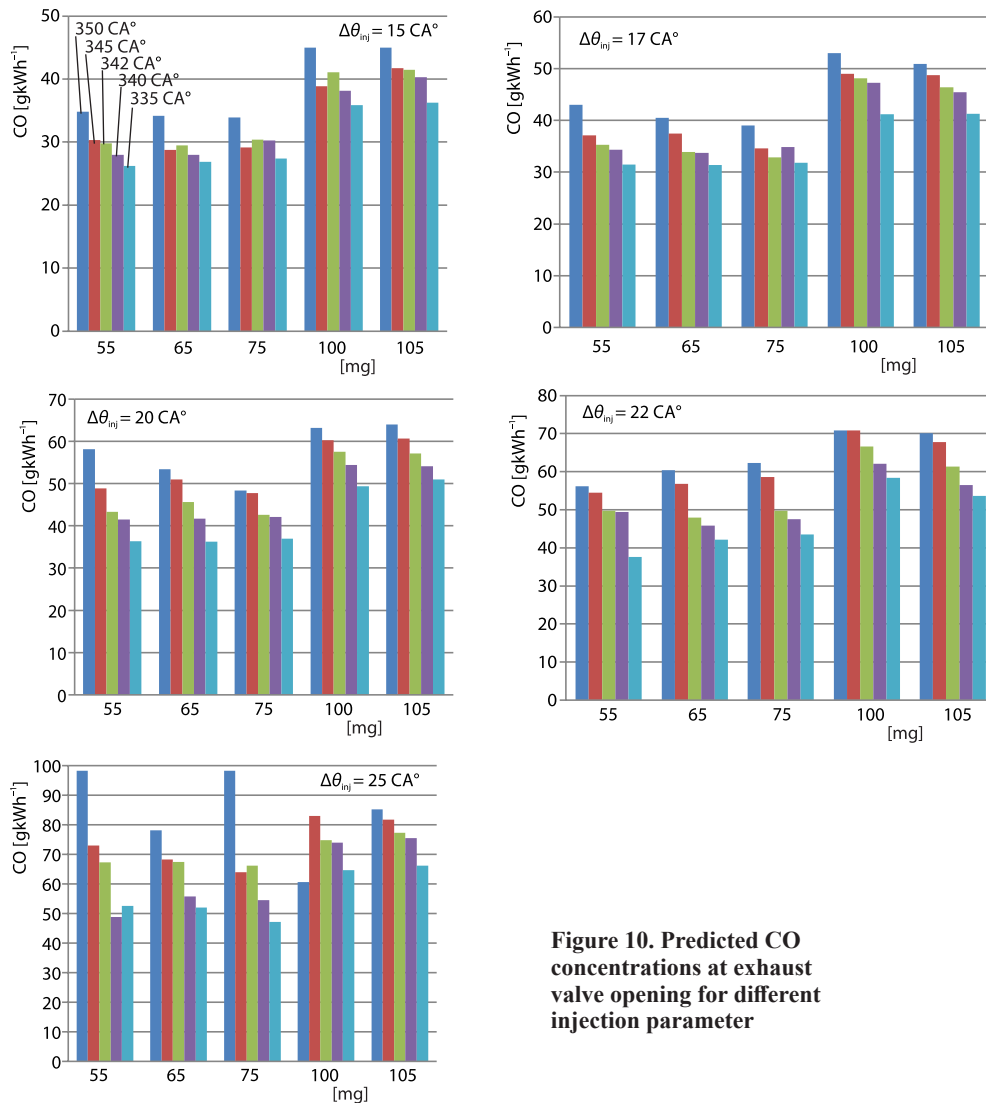


Figure 10. Predicted CO concentrations at exhaust valve opening for different injection parameter

Ignition delays seem to be more sensitive to injection timing and injection duration variations than combustion duration. Higher ignition delays can be obtained when more amounts of fuel have been injected.

The analysis of the numerical results concludes that for the same mass of fuel injected, are as follows.

- Advancing injection timing duration increase both averaged in-cylinder pressure peak and the NO_x levels with lower levels of CO at the exhaust.
- Advancing injection duration reduces both averaged in-cylinder pressure peak and the NO_x levels accompanied with higher CO levels at the exhaust.

A compromise seems to be necessary to get good performances with acceptable emission levels of NO_x and CO at the exhaust.

Nomenclature

A	– constant
A_{CO}	– constant
B	– constant
k	– turbulent kinetic energy
m_f	– fuel mass injected
N	– engine speed
P	– pressure
P_{max}	– maximum in-cylinder pressure
T	– temperature

T_{max}	– maximum in-cylinder temperature
t	– time

Greek symbols

α	– exponent for NO and NO _x relations
ε	– turbulent kinetic energy dissipation
θ_{inj}	– injection timing
$\Delta\theta_{inj}$	– injection duration

References

- [1] Golovitchev, V. I., *et al.*, The 3-D Diesel Spray Simulations Using a New Detailed Chemistry Turbulent Combustion Model, SAE Technical paper 00FL-447, 2000
- [2] Nordin, N., Complex Chemistry Modelling of Diesel Spray Combustion, Ph. D. thesis, Thermo-Fluid-Dynamics Laboratory, Chalmers University, Trondheim, Sweden, 2000
- [3] Heywood, J. B., *Internal Combustion Engine Fundamentals*, McGraw-Hill Inc., New York, USA, 1983
- [4] Gunter, P. M., *et al.*, *Simulating Combustion, Simulation of Combustion and Pollutant Formation for Engine-Development*, Springer-Verlag Berlin, Heidelberg, Germany, 2006
- [5] Ramos, J. I., *Internal Combustion Engine Modelling*, Hemisphere Publishing Corporation, New York, USA, 1989
- [6] Ferguson, C. R., Kirkpatrick, A. T., *Internal Combustion Engines*, 3rd ed., Applied Thermosciences, Wiley New York, USA, 2015
- [7] Amsden, A. A., *et al.*, The KIVA-II: *A Computer Program for Chemically Reactive Flows with Sprays*, Los Alamos, NM: LA-11560-MS, Los Alamos National Laboratory, Los Alamos, N. Mex., USA, 1989
- [8] Amsden, A. A., The KIVA-3: *A KIVA Program with Block-Structured Mesh for Complex Geometries*, Technical Report, Los Alamos National Laboratory, LA-12503-MS, Los Alamos, N. Mex., USA, 1993
- [9] Amsden, A. A., The KIVA-3V: *A Block-structured KIVA Program for Engines with Vertical or Canted Valves*, Technical Report, Los Alamos National Laboratory, LA-13313-MS, Los Alamos, N. Mex., USA, 1997
- [10] Amsden, A. A., The KIVA-3V: Released 2, Improvement to Kiva-3v, Technical Report, Los Alamos National Laboratory, LA-13608-MS, Los Alamos, N. Mex., USA, 1999
- [11] Reitz, R. D., Bracco, F. V., Mechanism of Atomization of a Liquid Jet, *Physics of Fluids*, 25 (1982), 10, pp. 1730-1742
- [12] Reitz, R. D., Bracco, F. V., Ultra-High-Speed Filming of Atomizing Jets, *Physics of Fluids*, 22 (1979), 6, pp. 1054-1064
- [13] Reitz, R. D., Bracco, F. V., *On the Dependence of Spray Angle and Other Spray Parameters on Nozzle Design and Operating Conditions*, SAE International Congress and Exposition, SAE Technical Paper No. 790494, Detroit, Mich., USA, 1979
- [14] Wu, K.-J., *et al.*, Measurements of Drop Size at the Spray Edge near the Nozzle in Atomizing Liquid Jets, *Physics of Fluids*, 29 (1986), 4, pp. 941-951
- [15] Han, Z., Reitz, R. D., Turbulence Modelling of Internal Combustion Engine Using RNG k - ε Models, *Combustion Science and Technology*, 106 (1995), 4-6, pp. 267-295
- [16] Reitz, R. D., Modelling Atomization Processes in High Pressure Vaporizing Sprays, *Atomization and Spray Technology*, 3 (1987), Jan., pp. 309-337
- [17] Bencherif, M., *et al.*, Pollution Duality in Turbocharged Heavy Duty Diesel Engine, *International Journal of Vehicle Design*, 50 (2009), 1-4, pp. 182-195
- [18] Ramalingam, S., *et al.*, Use of Antioxidant Additives for NO_x Mitigation in Compression Ignition Engine Operated With Biodiesel from Annon-a Oil, *Thermal Science*, 22 (2016), Suppl. 4, pp. S967-S972
- [19] Manickam, M. V., *et al.*, Effect of Steam Injection on NO_x Emissions and Performance of a Single Cylinder Diesel Engine Fuelled with Soy Methyl Ester, *Thermal Science*, 21 (2017), Suppl. 2, pp. S473-S479
- [20] Bencherif, M., *et al.*, Turbulence-Combustion Interaction in Direct Injection Diesel Engine, *Thermal Science Journal*, 18 (2014), 1, pp. 17-27
- [21] Bencherif, M., *et al.*, Turbulent Combustion Modelling in Compression Ignition Engines, Applied Mechanics, Behavior of Materials, and Engineering Systems, Lecture Notes Mechanical Engineering, Springer International Publishing Switzerland, New York, USA, 2017

- [22] Bencherif, M., *et al.*, A Novel NO_x Correlation for CI Engine Using Multidimensional Detailed Chemistry, *International Review of Mechanical Engineering*, 13 (2019), 5, pp. 1970-8734
- [23] Guzzella, L., Onder, C. H., *Introduction Modelling and Control of Internal Combustion Engine Systems*, Springer Heidelberg, Berlin, Germany, 2004
- [24] Robert J., *et al.*, *Chemically Reacting Flow Theory and Practice*, Wiley-Interscience, New York, USA, 2003
- [25] Senthil Kumar, M., *et al.*, A Comparative study of Different Methods of Using Animal Fat as a Fuel in a Compression Ignition Engine, *Journal for Engineering for Gas Turbines and Power*, 12 (2006), 8, pp. 907-914
- [26] Lounici, M. S., *et al.*, Towards Improvement of Natural Gas-Diesel Dual Fuel Mode: An Experimental Investigation on Performance and Exhaust Emissions, *Energy*, 64 (2014), Jan., pp. 200-211
- [27] Aklouche, F. Z., Model of the Diesel Engine Operating in Dual-Fuel Mode Fueled with Different Gaseous Fuels, *Fuel*, (2018), pp. 599- 606
- [28] Tazerout, M., *et al.*, A New Method to Determine the Start and end of Combustion in an Internal Combustion Engine Using Entropy Changes, *Int. J. Applied Thermodynamics*, 3 (2000), 2, pp. 49-55